Spontaneous Circular Motion of Microtubule Asters

Boyan Li
Department of Systems Biology, Harvard Medical School, Boston, Massachusetts 02115, United States
(Dated: May 19, 2024)

I present a simple non-equilibrium mean-field theory to describe the motion of the microtubule aster driven by the collective force of dyneins. In one dimension, the model predicts a phase transition of a symmetric aster from static to spontaneous directed motion. Critical values for dynein density and ATP consumption are explicitly calculated. In a viscoelastic system, this instability results in oscillations in one dimension and circular motion in two dimensions, with the latter being observed experimentally.

Microtubules (MTs) are important components of the cellular cytoskeleton and play a crucial role in various cellular functions including motility and the transport of intracellular cargo. These functions are facilitated by molecular motors, such as dyneins and kinesins, which exert pulling forces on MTs through ATP hydrolysis, inducing their movement [1]. Physically, MTs driven by motor proteins are considered classic examples of polar colloids and have been predicted to demonstrate collective behaviors, leading to the formation of asters, vortices, or spirals [2–4]. These collective phases have been experimentally observed in the motility assay, where purfied MTs are added to a glass surface grafted with motor molecules (see Fig. 1a) [5–7].

MTs within eukaryotic cells face restrictions imposed by the MT organizing center (MTOC), which ensures the radial growth of MTs [8]. These structure of asters is integral to mitosis and spatial distribution of organells and vesicles. The recent advancement of cell-free systems using undiluted Xenopus egg extracts has enabled the real-time imaging of aster growth under various perturbations while keeping the environment similar to in-vivo conditions [9]. Interestingly, when conducting MT motility assays within the egg extract, asters were observed to exhibit persistent circular motion, yet how such spontaneous motion emerged from collective behavior of dyneins remains elusive (see Fig. 1b) [10].

The collective behavior of motor molecules has been suggested to induce instability, leading to directed motion without external force [11] and oscillation under external elastic force [12–14]. Oscillation of mitotic spindles has been observed in C. elegans embryos and is thought to result from a combination of instability induced by dynein and elastic force generated by cortex-microtubule interactions [15, 16]. However, the behavior of a population of dyneins constrained by a microtubule aster has not been explicitly modeled. The absence of cortex in the egg extract system suggests that the elastic force arises not from cortex-microtubule interactions but potentially from the viscoelastic properties of the cytoskeletal network itself [17].

I begin by studying the 1D behavior of an aster of microtubules (MTs) by extending the model in [11], which describes a single MT. If the system is moving with velocity v, the Fokker-Planck equation can be written as:

$$\partial_t \rho_\pm(x) + v\partial_x \rho_\pm(x) = k_{\text{on}}\left[\sigma - \rho_\pm(x)\right] - k_{\text{off}}^\pm(x)\rho_\pm(x), \tag{1}$$

where $\rho_\pm$ is the density of dyneins bound to MTs to the left and right of MTOC, respectively (see Fig. 1a). Assuming the MTOC is located at $x = x_0$, then $\rho_+(x < x_0) = 0$, $\rho_-(x > x_0) = 0$. The sign of dyneins are determined by their natural walking directions. When $\rho_-(x) = 0$, the equation reduces to the single-MT scenario. Here, σ represents the density of total grafted dyneins, each of which can be in either the MT-bound state or the free state. k_{on} and k_{off} are the association and dissociation rate constant of dynein to MTs, respectively. While k_{on} is assumed to be constant, k_{off} depends on position x and thus differs for $\pm$. Note that (1) suggests that all the dyneins are rigidly coupled, ignoring spatial fluctuations, and thus the theory is mean-field. Due to the low Reynold number of cytoplasm, the inertial effect is generally negligible, and the force balance condition is

$$f_{\text{E}} = \xi_0 v - \int_{-\infty}^{\infty} \mathrm{d}x \left[\rho_+(x) f_+(x) + \rho_- f_-(x)\right], \tag{2}$$

in which $f_\pm(x)$ is the force generated by a dynein at x. Such force is determined by the binding energy $G(x)$, and $f = -\partial_x G(x)$. The binding energy has been considered periodic, i.e., $G(x + \ell) = G(x)$, where ℓ is the step size of the dynein (see Fig. 1a). Within each step size, the energy landscape is an asymmetric single-peak function [11, 18, 19]. Thus (2) can be simplified by integrating over one step size:

$$f_{\text{E}} = \xi v + \int_0^{\ell} \mathrm{d}x \left[\rho_+(x)\partial_x G_+(x) + \rho_- \partial_x G_-(x)\right], \tag{3}$$

where ξ is the drag coefficient of a MT unit with length 2ℓ. At equilibrium, the relation between k_{on} and k_{off} is governed by the detailed balance, and thus

$$k_{\text{off}}(x) = k_{\text{on}} e^{\beta[G(x) + \Delta\mu(x)]}. \tag{4}$$

$\Delta\mu$ is chemical potential difference between ATP and ADP. Note that ATP excitation only occurs at certain

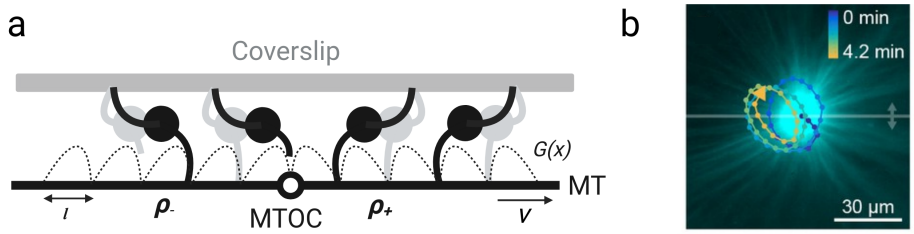

FIG. 1. (a) Schematics of the motility assay. The dashed lines are the periodic energy landscape. (b) Circular motion of the aster, adapted from [10].

configurations of the dynein and is thus dependent on x. Combining (1)-(4), a series solution can be obtained:

$$\rho_\pm = \sum_{n=0}^{\infty} \wp_n^\pm(x) v^n, \tag{5}$$

$$f_\mathrm{E} = f_0 + (\xi + f_1)v + \sum_{n=2}^{\infty} f_n v^n, \tag{6}$$

in which the following recursion relations is satisfied:

$$\wp_0^\pm = \frac{\sigma}{1 + e^{\beta\Delta\mu_\pm} e^{\beta G_\pm}}, \tag{7}$$

$$\wp_n^\pm = -\frac{1}{k_\mathrm{on}\sigma\wp_0^\pm}\partial_x \wp_{n-1}^\pm, \tag{8}$$

$$f_n \equiv f_n^+ - f_n^- = \int_0^\ell \mathrm{d}x \left(\wp_n^+ \partial_x G_+ + \wp_n^- \partial_x G_-\right). \tag{9}$$

Note that the energy landscapes to the left and right of the MTOC satisfy the following symmetry (see Fig. 1a):

$$G_+(x) = G_-(\ell - x), \quad \Delta\mu_+(x) = \Delta\mu_-(\ell - x). \tag{10}$$

Thus, for any functional $\mathcal{F}[G, \Delta\mu, G'^m, \Delta\mu'^m]$, $\mathcal{F}(x) - \mathcal{F}(\ell - x)$ is antisymmetric with respect to $\ell/2$ if m is even, and is symmetric if m is odd. Then $f_n = 0$ if n is even and $f_n \neq 0$ if n is odd. This gives rise to

$$\begin{aligned} f_\mathrm{E} &= (\xi + f_1)v + f_3 v^3 + \mathcal{O}(v^5) \\ &= (\xi + 2f_1^+)v + 2f_3^+ v^3 + \mathcal{O}(v^5) \end{aligned} \tag{11}$$

where $f_3 > 0$. (11) is analogous to the derivative of Landau-Ginzburg Hamiltonian of a magnet [20], and the criticality occurs at $\xi + 2f_1^+ = 0$. When $f_1^+ > -\xi/2$, the only solution to $f_\mathrm{E} = 0$ is $v = 0$ and thus the system is static. However, when $f_1^+ < -\xi/2$, due to the stability requirement that $\partial f_\mathrm{E}/\partial v > 0$, the solution is

$$v = \pm\sqrt{-\frac{\xi + 2f_1^+}{2f_3^+}} \tag{12}$$

which suggests that instability naturally emerges despite the aster is symmetric (see Fig. 2a).

In fact, in a single MT case,

$$f_\mathrm{E} = f_0^+ + (\xi_1 + f_1^+)v + f_2^+ v^2 + f_3^+ v^3 + \mathcal{O}(v^4) \tag{13}$$

The drag is primarily due to skin friction and is therefore proportional to the length of the microtubule (MT), i.e., $\xi \approx 2\xi_1$. Consequently, the spontaneous motion of a single polar MT also occurs when $f_1^+ < -\xi/2$, indicating that the critical behavior of a symmetric aster is similar to that of a single polar MT. The main difference is that f_0 and f_2 in the single-MT system are nonzero, which biases the f_E-v curve to one side (see Fig. 2b). Hence, the phase transition of the aster is analogous to paramagnet-to-ferromagnet transition while a single MT is analogous to liquid-to-gas transition. Therefore, the phase transition of the aster is analogous to a paramagnet-to-ferromagnet transition, while a single MT is analogous to a liquid-to-gas transition. The reason a symmetric aster exhibits instability as easily as an asymmetric MT is that the directed motion of the MT places dyneins on the opposite side in an unfavorable position, forcing them to detach from the MT (see Fig. 2c).

To explicitly determine the critical value, assume that $\Delta\mu$ follows

$$\Delta\mu(x) = \mu\left[\Theta(x - \ell + d) - \Theta(x - d)\right] \tag{14}$$

where Θ is the Heaviside step function. Then the critical dynein density is

$$\sigma_c = \frac{\xi k_\mathrm{on}}{\beta}\left[\frac{\mu}{8}(G'(d) - G'(\ell - d)) - \int_0^\ell \mathrm{d}x \frac{e^{\beta\Delta\mu} e^{\beta G} G'^2}{(1 + e^{\beta\Delta\mu} e^{\beta G})^3}\right]^{-1} \tag{15}$$

ATP level μ should be greater than a critical value μ_c to ensure σ_c to be positive, otherwise the system will remain static no matter how dense dyneins are grafted. As $f_n^+ \propto \sigma$ for all n, the critical behavior for σ is

$$\lim_{\sigma\to\sigma_c^+} |v| \propto \sqrt{\frac{\sigma - \sigma_c}{\sigma_c^2}} \tag{16}$$

To extend the above model to 2D, theoretically the dynamic behavior is determined by the following equations:

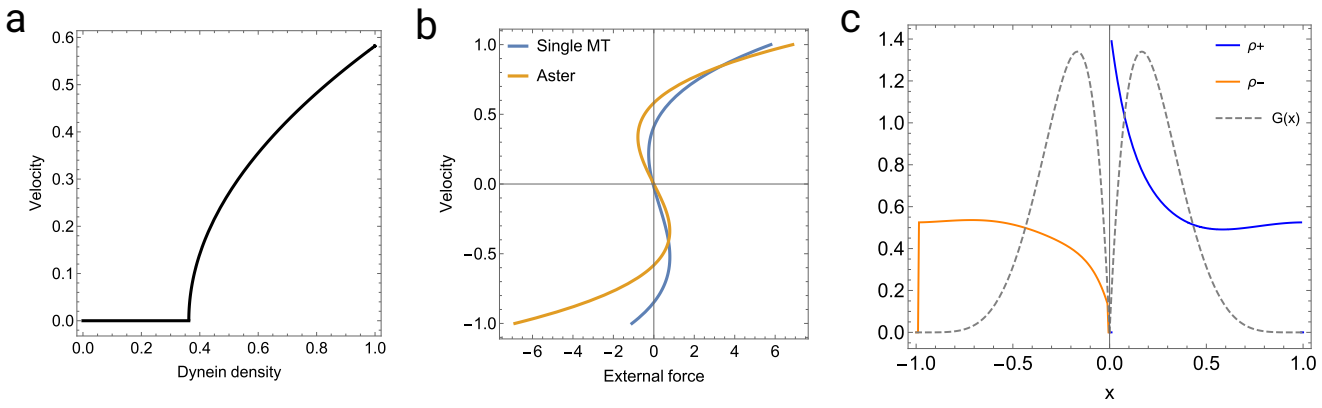

FIG. 2. (a) Steady-state velocity as a function of dynein density. (b) Velocity as a function of external force for single MT and aster. (c) $\rho_{\pm}(x)$ at $(-\ell, \ell)$, where MTOC is located at $x = 0$ and the aster has a positive velocity. Dyneins bound to the left half of MT are depleted.

$$\partial_t \rho(x,y) + \vec{v}\cdot\vec{\nabla}\rho(x,y) = k_{\rm on}(x,y)[\sigma - \rho(x,y)] - k_{\rm off}(x,y)\rho(x,y), \tag{17}$$

$$f_{{\rm E},\phi} = \xi v_\phi + \int_0^{2\pi} {\rm d}\theta\ \sin\theta \int_0^\infty {\rm d}r\ \rho(r,\theta)\partial_r G(r,\theta), \tag{18}$$

$$f_{{\rm E},R} = \xi v_R + KR + \int_0^{2\pi} {\rm d}\theta\ \cos\theta \int_0^\infty {\rm d}r\ \rho(r,\theta)\partial_r G(r,\theta). \tag{19}$$

Here, the origin of the system is the location of MTOC of an aster at equilibrium. There are two sets of coordinates, (r,θ) is the polar system of the aster, and (R,ϕ) is the polar system whose origin is the center of the aster orbit. $\theta = 0$ is the direction pointing to $R = 0$. K is the Hookean constant of the elastic force. The analysis of (17)-(19) will be described elsewhere. Here I provided a more qualitative analysis. In fact, regardless of inhomogeneity of MT distributions, dynein bound to MT of each direction should be expanded with a component of the velocity. Then (13) can be generalized as

$$\vec{f}_{D,\parallel}(\theta) = \cos\theta \sum_{n=0}^{\infty} f_n^+ (v\cos\theta)^n, \tag{20}$$

$$\vec{f}_{D,\perp}(\theta) = \sin\theta \sum_{n=0}^{\infty} f_n^+ (v\cos\theta)^n, \tag{21}$$

which are the parallel and perpendicular components of the force generated by dyneins bound to the MT that has an angle of θ to the velocity $\vec{v}$. Integrating over θ, $\vec{f}_{D,\perp}$ vanishes, and

$$\begin{aligned} f_{\rm E} &= \xi v + \int_0^{2\pi} {\rm d}\theta\ f_{D,\parallel}(\theta) \\ &= \left(\xi + \pi f_1^+\right) v + \frac{3\pi}{4} f_3^+ v^3 + \mathcal{O}(v^5) \end{aligned} \tag{22}$$

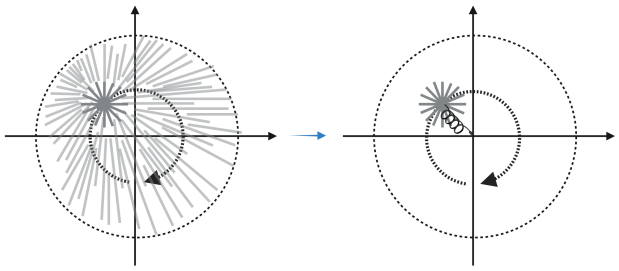

FIG. 3. Simplied picture of aster's circular motion. Only MTs attached to MTOC is considered, while the surrounding together provides a elastic force towards origin. Spring-like behavior of the aster has been reported [17].

(22) suggests that 2D case is almost the same as 1D, where the direction of force generated by dyneins are always in the same direction as $\vec{v}$. If a radial elastic force is applied to the aster while $\vec{v}$ is at steady-state, the radial component of $\vec{v}$ will ultimately vanish and the aster will undergo uniform circular motion (see Fig. 3). The circular motion can be considered as 1D directed motion on a circle, i.e., tangential instability. The radius of the circular motion has the relation $R \propto \sqrt{1/K}|\vec{v}|$.

In summary, I have demonstrated that an aster of MTs pulled by dyneins can undergo a static-to-instability phase transition. This transition is as likely to occur in

an aster as in a single polar MT due to the negative cooperativity of dyneins moving in opposite directions. Given the inherent symmetry of the aster, the transition is analogous to a paramagnet-to-ferromagnet transition, exhibiting a sudden jump in steady-state velocity as the external force changes continuously. If the relaxation time for dynein binding state transitions is fast and MTs are densely packed, the conclusions drawn from the 1D model can be readily extended to 2D. In this scenario, coupling the aster to a radial elastic force will naturally produce uniform circular motion, as observed in egg extract experiments. Experimentally, if the model is valid, the phase transition – either from static to circular motion or from $R = 0$ to a positive constant – can be achieved by increasing grafted dynein density over the critical value σ_c. The near-critical behavior of this transition is governed by a universal exponent of $1/2$.

I would like to thank Prof. Mehran Kardar for introducing the topics on criticality in phase transition and the dissipative dynamics, which inspires the formalization of this paper. I am also very grateful to Prof. Tim Mitchison who introduced to me this problem, and Natalia Orlovsky for useful discussions.

[1] D. Mizuno, C. Tardin, C. F. Schmidt, and F. C. MacKintosh, Nonequilibrium Mechanics of Active Cytoskeletal Networks, Science **315**, 370 (2007).

[2] K. Kruse, J. F. Joanny, F. Jülicher, J. Prost, and K. Sekimoto, Asters, Vortices, and Rotating Spirals in Active Gels of Polar Filaments, Phys. Rev. Lett. **92**, 078101 (2004).

[3] K. Kruse, J. F. Joanny, F. Jülicher, J. Prost, and K. Sekimoto, Generic theory of active polar gels: A paradigm for cytoskeletal dynamics, Eur. Phys. J. E **16**, 5 (2005).

[4] R. Voituriez, J. F. Joanny, and J. Prost, Generic Phase Diagram of Active Polar Films, Phys. Rev. Lett. **96**, 028102 (2006).

[5] T. Surrey, F. Nédélec, S. Leibler, and E. Karsenti, Physical Properties Determining Self-Organization of Motors and Microtubules, Science **292**, 1167 (2001).

[6] T. Sanchez, D. T. N. Chen, S. J. DeCamp, M. Heymann, and Z. Dogic, Spontaneous motion in hierarchically assembled active matter, Nature **491**, 431 (2012).

[7] Y. Sumino, K. H. Nagai, Y. Shitaka, D. Tanaka, K. Yoshikawa, H. Chaté, and K. Oiwa, Large-scale vortex lattice emerging from collectively moving microtubules, Nature **483**, 448 (2012).

[8] B. R. Brinkley, Microtubule Organizing Centers, Annu. Rev. Cell. Biol. **1**, 145 (1985).

[9] P. A. Nguyen, A. C. Groen, M. Loose, K. Ishihara, M. Wühr, C. M. Field, and T. J. Mitchison, Spatial organization of cytokinesis signaling reconstituted in a cell-free system, Science **346**, 244 (2014).

[10] J. F. Pelletier, C. M. Field, S. Fürthauer, M. Sonnett, and T. J. Mitchison, Co-movement of astral microtubules, organelles and F-actin by dynein and actomyosin forces in frog egg cytoplasm, eLife **9**, e60047 (2020).

[11] F. Jülicher and J. Prost, Cooperative Molecular Motors, Phys. Rev. Lett. **75**, 2618 (1995).

[12] F. Jülicher and J. Prost, Spontaneous Oscillations of Collective Molecular Motors, Phys. Rev. Lett. **78**, 4510 (1997).

[13] O. Campàs and P. Sens, Chromosome Oscillations in Mitosis, Phys. Rev. Lett. **97**, 128102 (2006).

[14] S. W. Grill, K. Kruse, and F. Jülicher, Theory of Mitotic Spindle Oscillations, Phys. Rev. Lett. **94**, 108104 (2005).

[15] J. Pecreaux, J.-C. Röper, K. Kruse, F. Jülicher, A. A. Hyman, S. W. Grill, and J. Howard, Spindle Oscillations during Asymmetric Cell Division Require a Threshold Number of Active Cortical Force Generators, Current Biology **16**, 2111 (2006).

[16] J. Howard and C. Garzon-Coral, Physical Limits on the Precision of Mitotic Spindle Positioning by Microtubule Pushing forces: Mechanics of mitotic spindle positioning, BioEssays **39**, 1700122 (2017).

[17] J. Xie, J. Najafi, R. Le Borgne, J.-M. Verbavatz, C. Durieu, J. Sallé, and N. Minc, Contribution of cytoplasm viscoelastic properties to mitotic spindle positioning, Proc. Natl. Acad. Sci. U.S.A. **119**, e2115593119 (2022).

[18] F. Jülicher, A. Ajdari, and J. Prost, Modeling molecular motors, Rev. Mod. Phys. **69**, 1269 (1997).

[19] Y. Ezber, V. Belyy, S. Can, and A. Yildiz, Dynein harnesses active fluctuations of microtubules for faster movement, Nat. Phys. **16**, 312 (2020).

[20] M. Kardar, *Statistical Physics of Fields*, 1st ed. (Cambridge University Press, 2007).